

A Fast Analysis of Electromagnetic Immunity Responses of RF Amplifier Circuit under CW/Digital-Modulation Schemes

Han-Chang Hsieh^{1,2}, Jay-San Chen², Chi-Hsueh Wang¹, Cheng-Nan Chiu³,
Ming-Shing Lin⁴, and Chun Hsiung Chen¹,

¹Department of Electrical Engineering and Graduate Institute of Communication Engineering, National Taiwan University, Taipei 106, Taiwan.

²Bureau of Standards, Metrology and Inspection (BSMI), Ministry of Economic Affairs, Taiwan.

³Department of Electrical Engineering, Da-Yeh University, Changhua 515, Taiwan.

⁴Department of Electrical Engineering, National Yunlin University of Science and Technology, Yunlin 640, Taiwan.

¹d95942001@ntu.edu.tw, ¹f86942008@ntu.edu.tw, ¹chchen@ew.ee.ntu.edu.tw

²Js.chen@bsmi.gov.tw, ³cnchiu@mail.dyu.edu.tw, ⁴starlin@yuntech.edu.tw

Abstract—This paper presents a fast analysis of the radiated susceptibility (RS) problem associated with the microstrip amplifier, which is illuminated by a uniform plane incident wave. By using the field-equations incorporated advanced design system (ADS) commercial circuit platform, the electromagnetic immunity responses of RF amplifier circuits, especially under digital modulation scheme, may efficiently be addressed. In this study, the simulated field-induced terminal voltages of microstrip single-stage RF amplifier circuit are presented and carefully examined with the results from measurements also included for validation.

Index terms — electromagnetic immunity, radiated susceptibility, RF amplifier circuit.

I. INTRODUCTION

The widespread use of wireless communication systems has significantly increased the environmental electromagnetic pollution. As a consequence, the amplitude of radio-frequency interference (RFI) picked up by wiring structures like cables and printed circuit board traces of electronic systems can be high enough to induce unexpected failures [1]. With the uptake of wireless devices and services, the problem concerning impact of electromagnetic (EM) coupling and interference on active circuits exposed to ambient radiation receives much attention [2]. Similar problems have also been faced with in amplifier systems, because RFI generated by the RF amplifier circuits can reach baseband circuits thus induce failures.

It is very difficult to analyze the undesired interference responses of RF amplifier circuits because the node current and voltage in an RF amplifier cannot be observed. Therefore, the establishment of an efficient simulation technique is a key to the analysis and prediction of the undesired interference.

Up to now, few papers have been addressed on the evaluation of the behavior of RF amplifiers under large RF illumination [3], [4]. In [3], [4], the electromagnetic (EM) solver has been used to combine with the equivalent sources of the linear microstrip sub-network induced by an incident plane wave. The amplifier circuit is then analyzed by the piecewise harmonic balance (HB) circuit solver. Because the

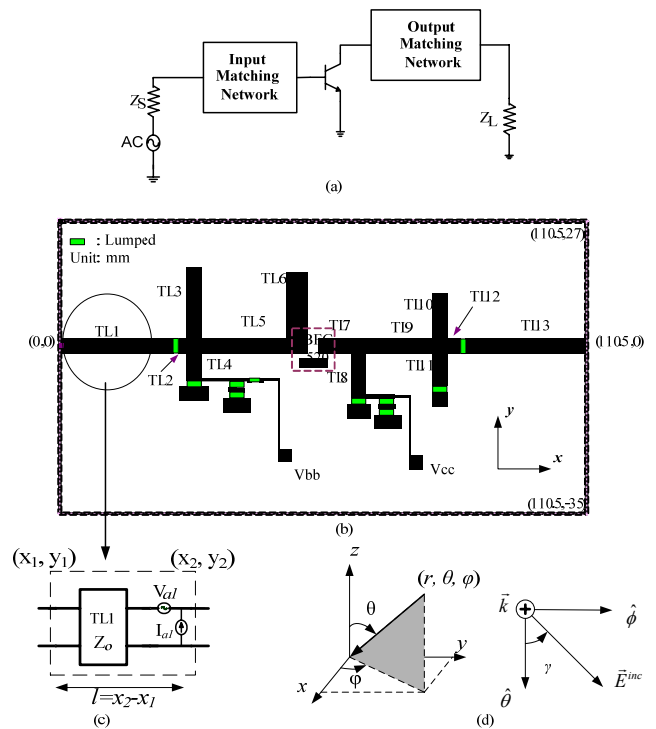


Fig. 1 Single-stage RF microstrip amplifier, (a) schematic diagram, (b) layout with transistor (BFG 520) and lumped elements removed, (c) equivalent circuit of a microstrip line element, (d) parameters to characterize the incident plane wave (θ, ϕ): incidence angles, γ : polarization angle).

method adopted by [3], [4] has used the EM field solver for simulating the microstrip network circuit, its efficiency in simulation would largely depend upon the speed of the EM field solver.

In this study, the recently developed equation-based hybrid fast method [5] will be used to analyze the field-influenced responses of the RF amplifier circuit on printed circuit board (PCB) which is excited by CW/digital-modulation sources

Table 1 Geometric parameters for microstrip line elements in Fig. 1(b).

Item	Width	Started point	Terminated point
TL 1	3.16	(0, 0)	(24, 0)
TL 2	3.16	(25, 0)	(28, 0)
TL 3	3.16	(29, 1.6)	(29, 16.6)
TL 4	3.16	(29, -1.6)	(29, -7.6)
TL 5	3.16	(30, 0)	(48, 0)
TL 6	4.5	(50, 1.6)	(50, 15.6)
TL 7	3.16	(55, 0)	(62, 0)
TL 8	3.16	(67, -1.6)	(67, -10.4)
TL 9	3.16	(70, 0)	(84, 0)
TL 10	3.16	(80, 1.6)	(80, 11.1)
TL 11	3.16	(80, -1.6)	(80, -8.7)
TL 12	3.16	(82, 0)	(85, 0)
TL 13	3.16	(86, 0)	(111.5, 0)

Unit: mm

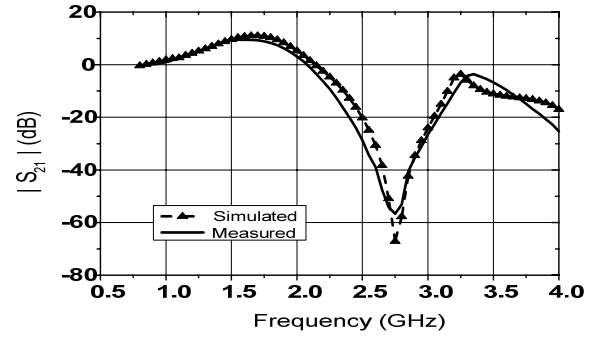


Fig. 2 Simulated and measured results for the S-parameters of the single-stage RF amplifier (Fig. 1).

(QPSK, QAM16, QAM32, and QAM64) and also illuminated by an external incident wave.

II. RF AMPLIFIER CIRCUIT CONFIGURATION

The transistor amplifier under consideration is implemented in PCB on FR4 substrate. It consists of input and output impedance matching networks, the BFG520 transistor, and other necessary circuits as shown in Fig. 1. The layout of this single-stage amplifier operated at 1.7 GHz is illustrated in Fig. 1(b). The microstrip interconnect is properly designed to meet the amplifier impedance matching conditions, and the corresponding width and length are given in Table 1. The S-parameters associated with this single-stage RF amplifier are depicted in Fig. 2, which implies that the amplifier presents a gain of 10 dB. Essentially, the measurement layout is also the same as in [5].

The single-stage amplifier circuit (Fig. 1) is mainly consisting of lumped elements, active components, and microstrip-line traces. Since the lumped elements (chipset resistors /capacitors) and active transistors are smaller in size when comparing with the wavelength, they are less affected by the incident wave field. Thus, the field-induced equivalent sources for the amplifier circuit on a PCB are mainly contributed from the microstrip-line elements, and the amplifier circuit may be regarded as a cascade of several microstrip-line elements as shown in Fig. 1.

The single-stage amplifier in Fig. 1 will be discussed by the fast method proposed in [5]. To be specific, the key steps in simulating the amplifier will be summarized in the following.

1) For each microstrip-line element, the parameters

associated with the location (x_i, y_i) , (specified in Table 1), the microstrip, and the incident plane wave are first substituted into the analytical equivalent source expressions (see [5] for details) so that one may calculate the field-induced equivalent sources (V_{ai}, I_{ai}) across the terminals of each microstrip element, such as in Fig. 1(c).

2) By incorporating these field-induced equivalent source expressions for all microstrip-line elements into the ADS circuit solver[6], and then combining these equivalent sources with the excitation sources (continuous wave or digital modulation source) of the circuit, one may use the same circuit solver to simulate the output terminal voltages and currents of the whole circuit.

In this study, the EM immunity related field-induced voltages of single-stage amplifier (Fig. 1) on FR4 substrate ($\epsilon_r = 4.6$, $h = 1.6$ mm) will be computed and compared with the ones by measurement. The amplifier is connected to the 50 Ω loads at the terminations. This amplifier circuit is excited by suitable CW/digital-modulation sources with a frequency 1.7 GHz. This amplifier is also illuminated by a plane wave, with $E_0 = 3$ V/m, $\gamma = \theta = \phi = 0^\circ$, over the frequency range 800- 4000 MHz, and its DC bias voltages are provided by the batteries for which $V_{cc} = 3$ V and $V_{bb} = 1$ V.

III. FIELD-INFLUENCED RESPONSES OF AMPLIFIER UNDER CONTINUOUS WAVE (CW) EXCITATION

The simulated and measured results characterizing the field-induced output terminal-voltages of the amplifier (Fig. 1) under CW excitation and illuminated by the plane wave are presented in Fig. 3. A good agreement among the simulated and measured results is observed. For comparison, Fig. 3 also includes the measured results with the absence of the incident wave ($E_0 = 0$ V/m). Especially, the incident plane wave may induce large out-band spurious response.

The influence of the incident plane wave on the linearity range of the single-stage amplifier, operating at 1.7 GHz with a CW source, is illustrated in Fig. 4. Obviously, the 1 dB

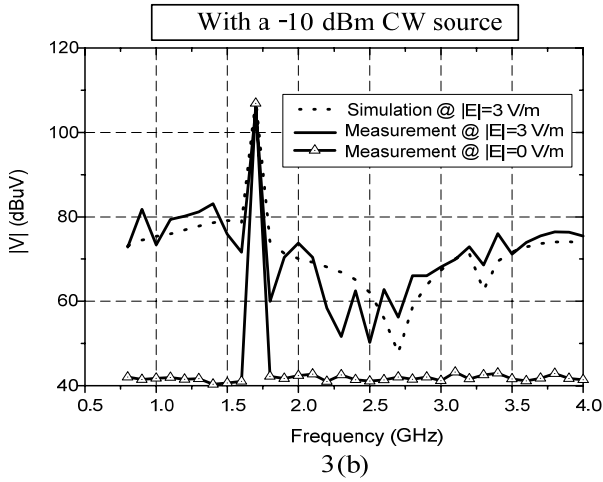
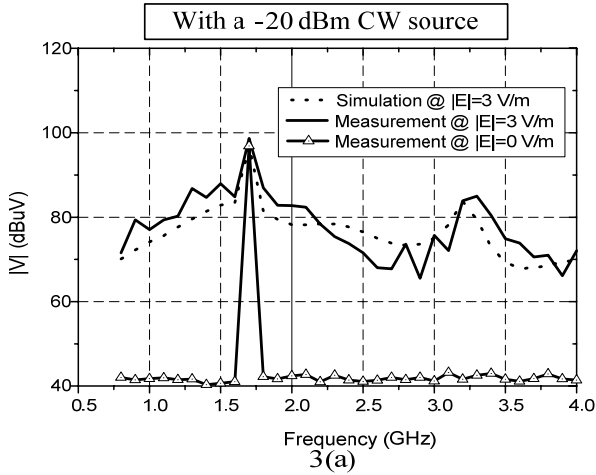


Fig. 3 Measured and simulated results for the field-induced output terminal voltages of the single-stage RF amplifier (Fig. 1). The amplifier is excited by a CW source of -20 dBm or -10 dBm at 1.7 GHz and is illuminated by an electric-field amplitude of $E_0=3$ V/m. (a) Y polarization ($\gamma=\theta=0^\circ$, $\phi=90^\circ$), (b) X polarization ($\gamma=\theta=\phi=0^\circ$).

compression point (P_{1dB}) is changed from $P_{in}=2.5$ dBm to $P_{in}=-1.6$ dBm. And, the gain of amplifier would be nonlinear while P_{in} is smaller than -35 dBm as shown in Fig. 4.

Fig. 5 shows the power gain versus amplifier input power subject to different plane wave strengths as simulated on the ADS platform. Here, the field-induced voltages at amplifier terminal point are presented and compared for various incident waves with $\gamma=\theta=\phi=0^\circ$. Note that significant power degradation at the amplifier output is observed due to the external plane wave illumination of strength 10, 50, and 100 V/m. When the amplifier is excited by the -8 dBm CW source, and illuminated by the external wave strength of 100 V/m, the output gain is degraded more than 18 dB. The power degradation is likely due to the variation in V_b voltage of amplifier which is changed from 73 mV to 28 mV. Because

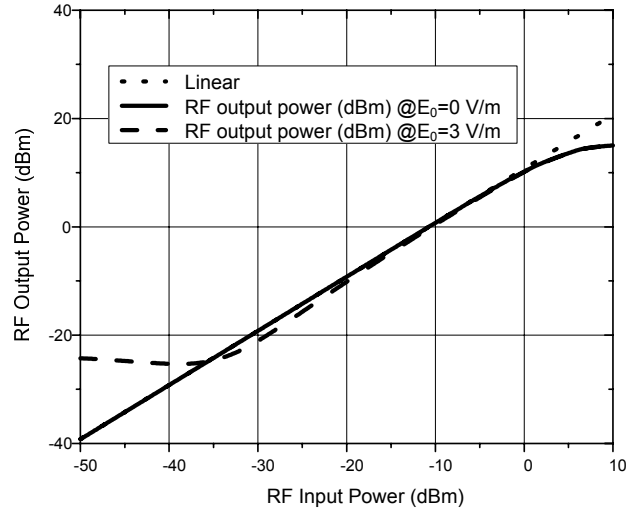


Fig. 4 Linearity range of the single-stage amplifier (Fig. 1).

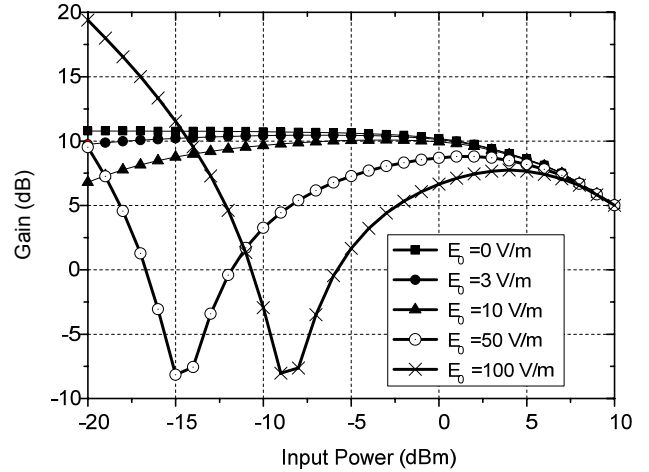


Fig. 5 Simulated gain versus input power for the single-stage amplifier (operating at 1.7 GHz) illuminated by an external plane wave at 1.7 GHz.

the field-induced voltage at transistor input terminal point (V_b) is significantly changed, it would have a critical impact on the amplifier circuitry.

IV. RADIATED SUSCEPTIBILITY SIMULATION UNDER DIGITAL MODULATION SCHEME

The influence on the digital-modulated output terminal voltages of the RF microstrip amplifier, which is illuminated by the external plane wave, would be an important topic in the EMC issue. Here, the constellation diagram is the most interesting one in presenting the substantial changes in the amplifier performance, which is excited by BPSK, QPSK, and QAM16 sources. By using the co-simulation circuit solver, the

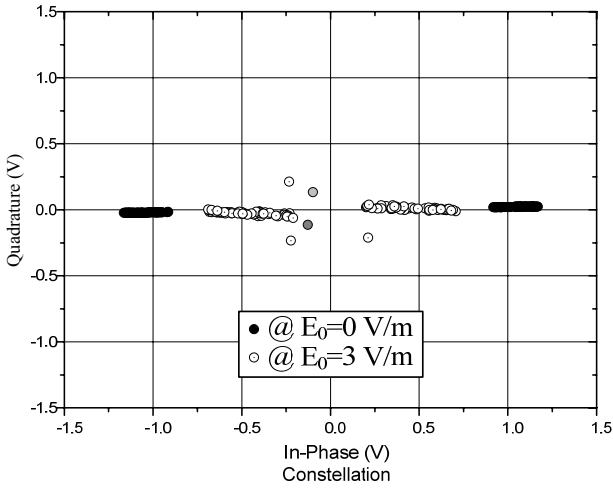


Fig. 6 Simulated results for the constellation diagram of the single-stage amplifier (operating at 1.7 GHz), which is excited by a BPSK source of (-10 dBm, 2 Mb/s, $f_c=1.7$ GHz) and is illuminated by an incident plane wave of amplitude $E_0=0$ V/m or 3 V/m, $f=1.701$ GHz, $\gamma = \theta = \phi = 0^\circ$.

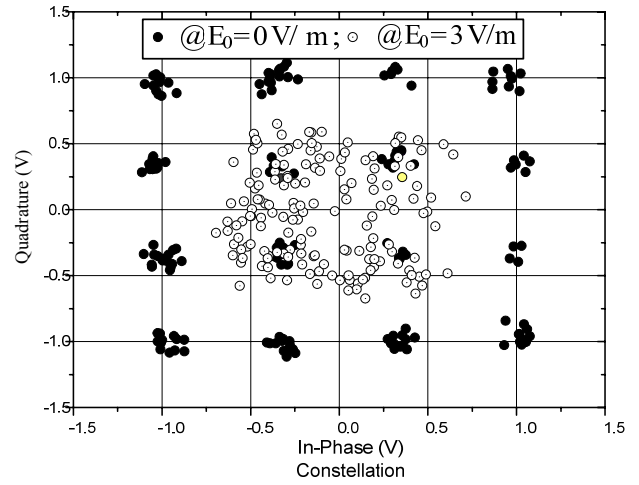


Fig. 8 Simulated results for the constellation diagram of the single-stage amplifier (operating at 1.7 GHz), which is excited by a QAM-16 source of (-10 dBm, 2 Mb/s, $f_c=1.7$ GHz) and is illuminated by an incident plane wave of amplitude $E_0=0$ V/m or 3 V/m, $f=1.701$ GHz, $\gamma = \theta = \phi = 0^\circ$.

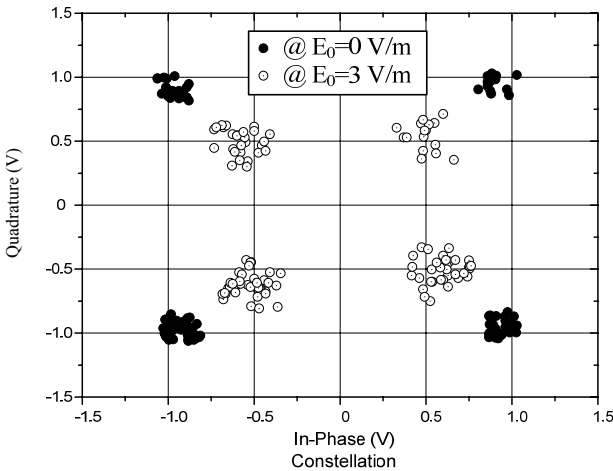


Fig. 7 Simulated results for the constellation diagram of the single-stage amplifier (operating at 1.7 GHz), which is excited by a QPSK source of (-10 dBm, 2 Mb/s, $f_c=1.7$ GHz) and is illuminated by an incident plane wave of amplitude $E_0=0$ V/m or 3 V/m, $f=1.701$ GHz, $\gamma = \theta = \phi = 0^\circ$.

fast method [5] will be used to characterize the radiated susceptibility problem associated with the RF amplifier which is fed by the BPSK, QPSK, and QAM16 digital modulation sources and is also illuminated by the external incident wave field.

With the external plane wave-field illumination ($E_0=0$ or 3 V/m), the constellation diagrams of the amplifier are illustrated in Figs. 6, 7, and 8. Specifically, Figs. 6, and 7

show the simulated results for the constellation diagram of the RF amplifier (operating at 1.7 GHz), which is excited by BPSK, and QPSK sources of (-10 dBm, 2 Mb/s, $f_c=1.7$ GHz) and is also illuminated by an incident plane wave of amplitude $E_0=0$ or 3 V/m, $f=1.701$ GHz, $\gamma = \theta = \phi = 0^\circ$. Note that in Figs. 6 and 7, the locations of the constellation signal of the amplifier has been moved by the external plane wave. Since the locations are still inside the noise margin, the output signals (both BPSK and QPSK) of amplifier could be demodulated by the receiver-circuit.

Till now, only the constant amplitude-modulated signals have been addressed. Next, our focus would be on the non-constant envelope QAM16 scheme which has in-phase and quadrature components that are modulated by cosine and sine functions. The corresponding simulated QAM16 constellation signals of the amplifier, with and without external wave-field illumination, are plotted in Fig. 8. With plane wave illumination ($E_0 = 3$ V/m), the QAM16 constellation signals would be mixed up at the output of the RF amplifier. Since the locations of signals have been moved over the noise margin, the demodulation of amplifier QAM16 signals would be quite difficult or even impossible.

Finally, shown in Table II are the error vector magnitude (EVM) values [5] for the amplifier (with QPSK, QAM16, QAM32, and QAM64 sources) which is illuminated by the uniform plane wave of frequency 1.701 GHz with the field amplitude of $E_0=0$ or 3 V/m. Here, the distance between constellation points are so short that QAM16, QAM32, and QAM64 are expected to be more sensitive to the external plane wave.

Table 2 Simulated results for the EVM of the single-stage amplifier (operating at 1.7 GHz), which is excited by several digital modulation sources and is illuminated by an incident plane wave of amplitude $E_{\bar{0}}=0$ or 3 V/m, $f=1.701$ GHz, $\gamma = \theta = \psi = 0^\circ$.

	EVM_{rms}	
	$E_{\bar{0}}=0$ V/m	$E_{\bar{0}}=3$ V/m
QPSK	5.8 %	14.8 %
QAM 16	6.5 %	16.3 %
QAM 32	8.8 %	15.9 %
QAM 64	5.7 %	13.4 %

V. CONCLUSION

The electromagnetic immunity problem associated with the single-stage microstrip amplifier in the nonlinear region has been carefully discussed. The constellation signals of the digital-modulated RF amplifier with and without external wave illumination are investigated. Due to the use of efficient equation-based fast method in simulation, the radiated susceptibility responses of the RF amplifier, including each node-voltage information of amplifier, may easily be predicted in the circuit design stage.

ACKNOWLEDGMENT

This work was supported by the Excellent Research Projects of National Taiwan University, NTU-ERP-98R0062-AE00-00, NSC 99-2221-E-212-002, and NSC-98-2221-E-224-011-MY2.

REFERENCES

- [1] C. R. Paul, "Introduction to Electromagnetic Compatibility," New York: Wiley, 1992.
- [2] E. S. Siah, J. L. Volakis, D. Pavlidis, and V. V. Liepa, "Electromagnetic analysis of plane wave illumination effect onto passive and active circuit topologies," *IEEE Antennas Wireless Propag. Lett.*, vol. 2, no. 1, pp. 230-233, 2003.
- [3] V. Rizzoli, A. Costanzo, and G. Monti, "General electromagnetic compatibility analysis for nonlinear microwave integrated circuits," in *IEEE MTT-S Int. Microw. Symp. Dig.*, 6-11 June 2004 vol. 2, pp. 953-956.
- [4] T. Yang, Y. Bayram, and John L. Volakis, "Hybrid analysis of electromagnetic interference effects on microwave active circuits within cavity enclosures," *IEEE Trans. on Electromagn. Compat.*, vol. 52, no. 3, pp. 745-748, August 2010.
- [5] H. C. Hsieh, C. N. Chiu, M. S. Lin, C. H. Wang, and C. H. Chen, "An equation-based hybrid method for predicting radiated susceptibility responses of RF/Microwave circuits," to be published in *IEEE Trans. on Electromagn. Compat.*.
- [6] <http://eesof.tm.agilent.com/>